

# Investigation of the relationship between current filament movement and local heat generation in IGBTs by using modified avalanche model of TCAD

Takeshi Suwa

Toshiba Electronic Devices & Storage Corporation, Kawasaki, Japan

Email: takeshi.suwa@glb.toshiba.co.jp

**Abstract**—For development of high voltage power devices, it is very important to understand local heat generation phenomena of current filaments especially for reliability designs. Current filaments mean high density currents flow only in some parts of active cells and induce large heat generation locally. They appear when excessive current flows for some reasons during device switching. The aim of this paper is to clarify the following by using a modified avalanche model: The local lattice temperature dependence of impact ionization coefficients is a main factor in current filament movements, and the movements significantly suppress local heat generation. In particular, this tendency becomes even stronger when the ambient temperature is low and after the depletion layer reaches the buffer layer on the back surface side of IGBTs.

**Keywords**—*IGBT, current filament, self-heating, avalanche model, Impact Ionization model*

## I. INTRODUCTION

Since power semiconductor devices such as IGBTs include instability [1], currents may not flow evenly throughout the device under certain conditions. If the currents locally flow and the current density increases, the local lattice temperature of silicon increases mainly due to Joule heat (self-heating), and the risk that the materials of the device melt and break increases. In other words, even under the condition that there is no problem in terms of energy if currents flow uniformly, there is a possibility of thermal breakdown for local and large current density. When developing a device, it is necessary to prevent local heat generation within the guaranteed operating range or to design so that the device will not be destroyed even if it occurs.

The phenomenon in which large local currents flow is called current crowding and creates local hot spots [2][3]. There are two types of current concentration: one in which a large current flows only at structural defects in termination regions or cell regions, and the other in which currents in cell regions gather and flow only in a part of cell regions. The latter, so-called current filaments, is due to device instability and is associated with snapback characteristics. The current filaments may travel within the cell area, hit the termination area, or be trapped in the defect area. The phenomena has been investigated by both actual measurements [4][5] and Technology CAD (TCAD) simulations [6][7].

If it is necessary to take care of short-circuit, overcurrent turn-off and unclamped inductive switching (UIS) phenomena in device developments, the current filament should be given special attention as it is directly related to device destruction. This work focuses on the current filament during overcurrent turn-off phenomenon [8]. The overcurrent turn-off phenomenon is that when IGBT turns off, a current several

times the rated current flows for some reasons. Generally, even in that case, if currents flow uniformly through the whole device, the device is not thermally destroyed.

Some current filaments may be formed depending on the device operating conditions, and may freely move three-dimensionally in the cell region and interfere with each other. Since it is difficult to actually observe how they interfere with each other, it is common to investigate them by simulations. If current filaments become pinned or their movements are restricted for some reasons, parasitic NPN structures on the surface region of cells will turn on and the device will be destroyed [8]. Conversely, it is also used to inspect unacceptable defects in the device structure [2].

TCAD simulations of the current filament are performed with a structure in which several tens to several hundreds of two-dimensional cell structures are connected and arranged (so-called multi-cell structure) [9], a structure in which a termination structure is added, or structures in which they are combined in a circuit. Depending on the purpose of the simulation, a defect model may be included in a part of the structure, or a multi-cell structure may be formed in three dimensions. Normally, it is necessary to perform calculation in consideration of self-heating, and set thermal boundary conditions on the front and back sides of the device and boundary conditions on the lateral surface of the device. If the lattice temperature of silicon reaches the melting temperature of silicon even in part, or if the parasitic NPN structure is apparently turned on and feedback is applied [8], it is estimated that the device has been destroyed in TCAD simulation. Therefore, the boundary conditions are very important in current filament simulations and should be determined to reproduce the tendency of operating conditions when the actual device fails.

The trigger for current filamentation in actual devices is subtle differences in snapback characteristics due to subtle structural differences between adjacent cell structures. On the other hand, in TCAD simulation, it is caused by subtle differences in the mesh structures and numerical calculations. Although there are differences in triggers, it is common to generate current filaments in TCAD simulation to investigate the relationship between the behavior of current filaments and the device destruction, and utilize the results for actual device development. However, it is desirable that the gate voltage and lattice temperature dependences of the snapback characteristic in TCAD simulation are almost the same as the actual device.

The movement of the current filament in the device is largely influenced by the lateral electric field caused by the imbalance of the carrier density on the left and right sides of the filament and the difference in the impact ionization coefficient due to the local difference in the lattice temperature [2]. The degree of their influence strongly depends on the circuit conditions and the ambient temperature.

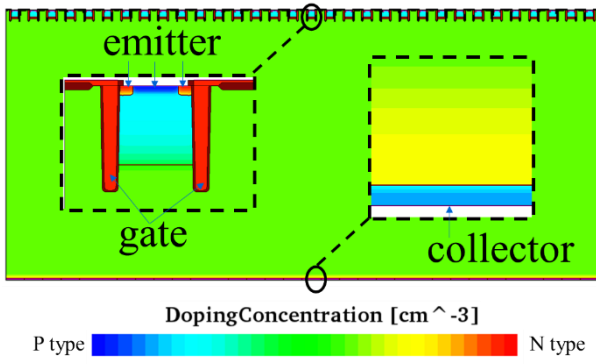


Fig. 1: Schematic view of the simulated structure (IGBT 32cells). The two figures surrounded by dotted lines are enlarged views of the front side surface and the back side surface.

## II. TARGETS AND SIMULATION APPROCH

In this study, overcurrent turn-off phenomena are simulated by Synopsys TCAD with thermodynamic model and periodic boundary condition for lateral sides. The thermal boundary conditions on the surface and back sides of the device are those that correlate well with the tendency of the breakdown strength of the actual device. The simulated structure has 32 cells arranged side by side as shown in Fig. 1. As the impact ionization model, "New University of Bologna Impact Ionization Model" (UniBo2) [10] is selected, which can reproduce the effect on the electrical characteristics even at high lattice temperatures. The model reads:

$$\alpha(F_{ava}, T) = \frac{F_{ava}}{a(T) + b(T) \exp \left[ \frac{d(T)}{F_{ava} + c(T)} \right]}$$

where the coefficients  $a$ ,  $b$ ,  $c$ , and  $d$  are polynomials of local lattice temperature  $T$  and  $F_{ava}$  is the driving force for impact ionization. When current filamentation occurs, the impact ionization coefficients in the current filament region and the impact ionization coefficients in the other regions become significantly different according to this equation. This is because the current filament has high carrier densities and generates a large amount of self-heating.

Furthermore, a modified UniBo2 model is implemented by using Physical Model Interface (PMI) [11] which is an application interface of Sentaurus™ Device. This model is basically UniBo2 model, however the lattice temperature variables  $T$  are always forced to be equal to the ambient temperature, and impact ionization coefficients do not depend on the local lattice temperature changes (hereinafter called PMI model). By comparing the overcurrent turn-off results calculated with each model, it is possible to clarify how much the local lattice temperature dependence of the impact ionization coefficients contributes to the current filament movements and local heat generation.

Fig. 2 shows DC-like breakdown characteristics calculated at each ambient temperature  $T_{amb}$  for gate-emitter voltage  $V_{ge}=0(V)$  with the above two avalanche models. From the figure, leakage currents are fixed at each  $T_{amb}$ , and the results of the breakdown voltage for each PMI model are

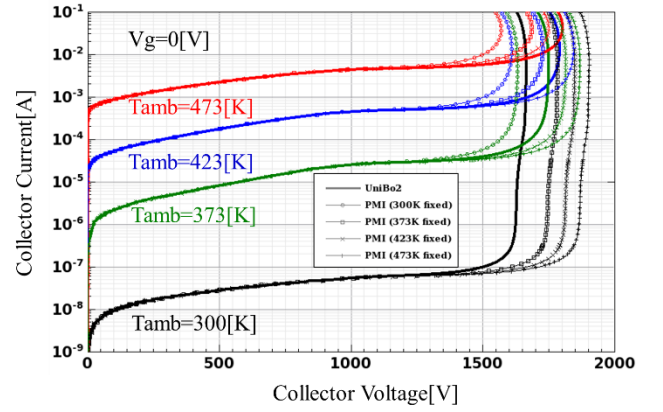


Fig. 2: DC-like breakdown characteristics calculated at each ambient temperature  $T_{amb}$  for gate-emitter voltage  $V_{ge}=0(V)$  with UniBo2 model (lines) and modified avalanche model (PMI model, lines with symbol).

close to the breakdown voltage of the original UniBo2 model according to the fixed lattice temperature. Since the leakage currents increase and the seed currents increase as  $T_{amb}$  rises, the breakdown voltage of each PMI model is slightly smaller than the breakdown voltage of UniBo2 model. From these calculation results, it can be confirmed that the PMI model is implemented as intended. Because a self-heating model is not taken into consideration in this calculation, the results of the UniBo2 model at each  $T_{amb}$  and the results of the PMI model in which the lattice temperature variables  $T$  are fixed at the corresponding  $T_{amb}$  are in agreement. Therefore, they are not shown in the figure.

## III. RESULTS AND DISCUSSION

Fig. 3 shows simulated overcurrent turn-off waveforms at gate resistance  $R_g=1(\Omega)$  and  $T_{amb}=300(K)$ . From Fig. 3(a), when  $V_{ge}$  decreases and reaches about a threshold voltage, the emitter electron current  $|I_{e\_electron}|$  becomes almost zero. In this case, the collector-emitter voltage  $V_{ce}$  and the collector current  $I_c$  are still large, so that dynamic avalanche occurs [12][13]. Fig. 3(b) shows the relationship between the maximum value of Si lattice temperatures at each time ( $LT_{max\_Si}$ ) and the regions 1 to 4. Each region is divided according to the change of  $LT_{max\_Si}$  waveform. The changes are caused by the current filaments generations, movements, and disappearances, which are shown in Fig. 4. From the figures, it can be seen that although current filaments are not generated in the region 2, they are being generated in the region 3. At the beginning of the region 4, thick and low-density current filaments are generated and disappear, and grow into thin and high-density filaments. As the filament moves, the mesh points of high lattice temperature, which are displayed in red, have a distribution that is dragged in the lateral direction.  $LT_{max\_Si}$  waveforms in Fig. 3 are jagged as the hottest current filament moves between cells. As can be seen from Figs. 3 and 4, after  $V_{ce}$  waveforms enter the plateau, that is, after the depletion layer extends and reaches the buffer layer on the back side, the jaggedness of the waveform, that is, the movement of the current filament becomes blunt.

Fig. 5 shows a comparison of overcurrent turn-off waveforms calculated with UniBo2 and PMI model.  $LT_{max\_Si}$  with the PMI model (red line) is less jagged, and the maximum point of  $LT_{max\_Si}$  waveform, that is, the

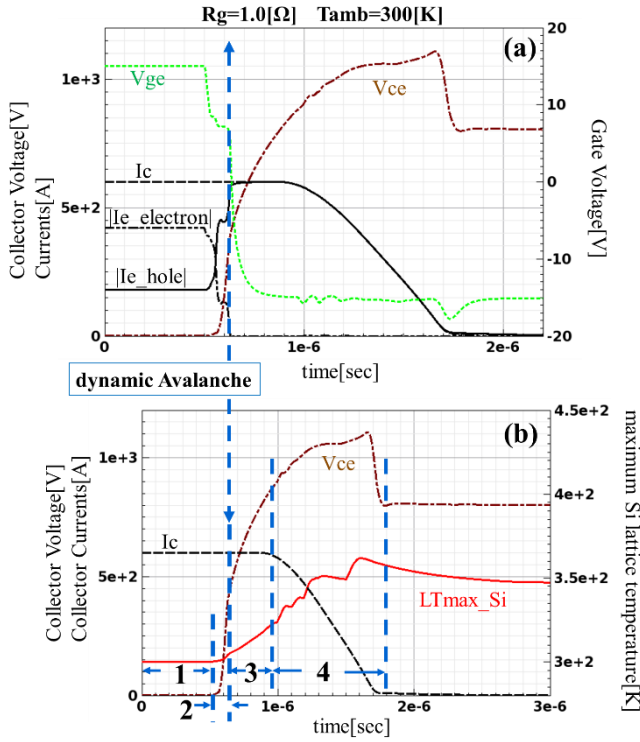


Fig. 3: Overcurrent turn-off simulation waveform calculated with UniBo2 model. The relationship between the waveforms and the cut off timing of the channel current (a) and the relationship between the maximum value of Si lattice temperatures ( $LT_{max\_Si}$ ) and the regions 1 to 4 (b).  $T_{amb}$  represents ambient temperature.

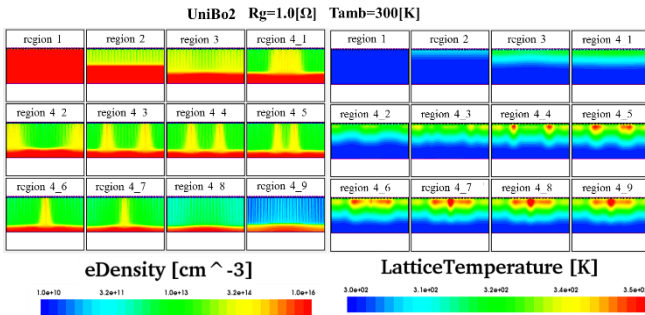


Fig. 4: Distributions of electron density (left) and lattice temperature (right) calculated with UniBo2 model corresponding to regions 1 to 4 in Fig. 3 (b). The figures for Region 4 are shown divided into approximately 9 parts in time (4\_1 to 4\_9).

maximum lattice temperature in whole turn-off phenomena becomes higher. This means that the local temperature dependency of the impact ionization coefficients greatly contributes to the current filament movements, and the smaller the movements, the larger the local heat generation. In other words, the local increase in the lattice temperature and the phonon scattering leads to the local decrease in the impact ionization coefficients, and as a result, the current filament movements to next cells are greatly promoted. From Fig. 6, it can be seen that the movement of the electron density and the local heat are smaller in PMI model results. As can be seen from Figs. 5 and 6, after  $V_{ce}$  waveforms enter the plateau, that is, after the depletion layer extends and reaches the buffer layer on the back side, the difference in  $LT_{max\_Si}$  becomes large. Therefore, in the region where the

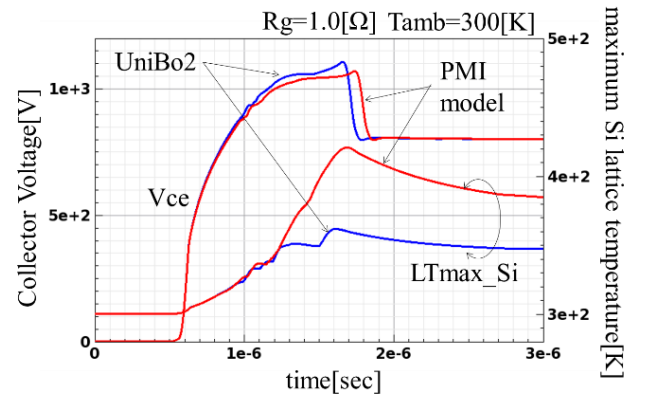


Fig. 5: Comparison of the waveforms calculated with UniBo2 model (blue lines) and an avalanche model created by using PMI (red lines). The latter model is based on UniBo2 model, but is modified to have no local lattice temperature dependence.

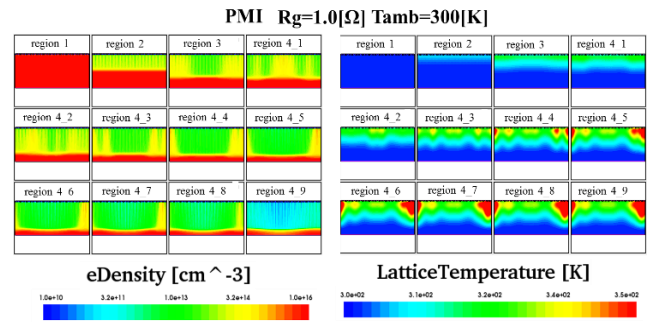


Fig. 6: Distributions calculated with PMI model under the same conditions as in Fig. 4.

heat generation is the highest in this phenomenon, the local lattice temperature dependence of the impact ionization coefficients has the greatest influence on the movements of current filaments and the suppression of heat generations.

Figs. 7(a) and 7(b) show  $T_{amb}$  dependences of overcurrent turn-off waveforms for a small and large  $R_g$ , respectively. When  $R_g$  is small and  $T_{amb}$  is not high, the filaments start moving at an earlier timing and suppress heat generation, however since they travel a long distance, they tend to be caught by structural defects in the actual system. This is one of the reasons that the measurements of overcurrent endurance vary greatly depending on the samples to be measured. In this case, the calculations with PMI model result in large local heat generation because the filament movements are suppressed for a long time. At  $T_{amb} = 423(K)$ , impact ionization is weak overall, therefore no current filament is generated, and the results are almost the same in both models. From Fig. 8, the hottest filament for a large  $R_g$  with PMI model does not move as if it were pinned and the local heat generation is large even for a short time. This is because under this operating condition, since current filaments are formed after  $V_{ce}$  waveforms enter the plateau, the movements of current filaments are almost determined by the local lattice temperature dependence of the impact ionization coefficients.

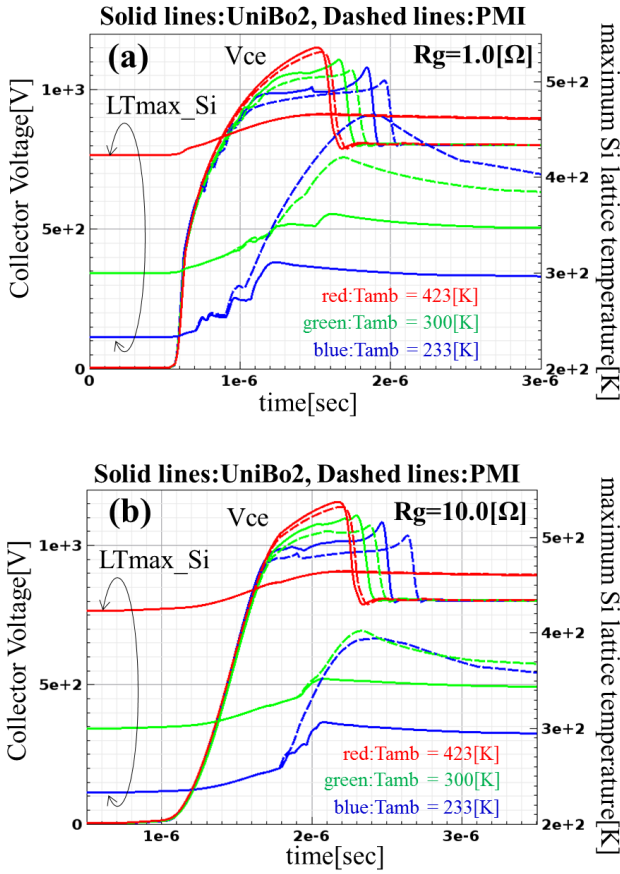


Fig. 7: Ambient temperature dependence of waveforms calculated with each model (Solid lines: UniBo2 model, dashed lines: PMI model) for (a)  $R_g=1.0(\Omega)$  and (b)  $R_g=10.0(\Omega)$ .

#### IV. CONCLUSION

In order to clarify that the local temperature dependence of the impact ionization coefficients is the main factor of current filament movements, the calculation results of the overcurrent turn-off phenomena using UniBo2 model were compared with the calculation results using PMI model. PMI model is based on UniBo2 model, however is a model modified by PMI so that it does not depend on local changes in the lattice temperature. Since current filament movements suppress local heat generation, if the movements are suppressed for some reasons, local heat generation will increase. The current filament movements also depends on the ambient temperature and the gate resistance, and if the ambient temperature is high to some extent, the current filaments are not generated from the beginning. If the ambient temperature is low and the gate resistance is low, current filaments will move a lot. In overcurrent turn-off phenomena, though large heat is generated after the collector voltage enters the plateau, the current filaments hardly move during this period in the calculation using PMI model, and heat generation becomes very large. In other words, the current filaments are almost driven by the difference in impact ionization coefficients due to the difference in lattice temperature between adjacent cells.

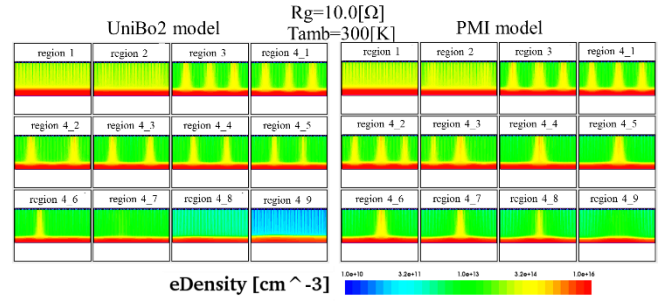


Fig. 8: Comparison of electron density distribution calculated with each model for  $R_g=10.0(\Omega)$ . The acquired timing of each figure is the same filaments conditions as the regions 1 to 4 in Figs. 3 and 4.

#### ACKNOWLEDGEMENT

I am grateful to K. Nakamura, T. Matsudai and S. Hayase for useful discussion. Company names, product names, and service names may be trademarks of their respective companies.

#### REFERENCES

- [1] A. Blicher, "Field-Effect and Bipolar Power Transistaer Physics", Academic Press, 1981, pp. 186–190.
- [2] T. Tamaki, Y. Yabuuchi, M. Izumi, N. Yasuhara and K. Nakamura, "Numerical study of destruction phenomena for punch-through IGBTs under unclamped inductive switching," Microelectronics Reliability, Vol. 64, September 2016, pp. 469–473.
- [3] Z. Chen, K. Nakamura and T. Terashima, "LPT(II)-CSTBT<sup>TM</sup>(III) for High Voltage Application with Ultra Robust Turn-off Capability Utilizing Novel Edge Termination Design," Proc. ISPSD 2012, pp. 25–28.
- [4] K. Endo et al., "Direct Photo Emission Motion Observation of Current Filaments in the IGBT under Avalanche Breakdown Condition," Proc. ISPSD 2016, pp. 367–370.
- [5] R. Bhojani, J. Kowalsky, J. Lutz, D. Kendig, R. Baburske, H. J. Schulze and F. J. Niedernostheide, "Observation of Current Filaments in IGBTs with Thermoreflectance Microscopy," ISPSD 2018, pp. 164–167.
- [6] Y. Mizuno, R. Tagami and K. Nishikawa, "Investigateions of Inhomogeneous Operation of IGBTs under Unclamped Inductive Switching Condition," Proc. ISPSD 2010, pp. 137–140.
- [7] M. Tanaka and A. Nakagawa, "Simulation studies for short-circuit current crowding of MOSFET-Mode IGBT," Proc. ISPSD 2014, pp. 119–122.
- [8] A. Muller-Dauch, F. Pfirsch, M. Pfaffenlehner and D. Silber, "Source Side Thermal Runaway of Trench IGBTs, Dependence on Design Aspects," ISPSD 2006, pp. 1–4.
- [9] M. Tanaka and A. Nakagawa, "Growth of short-circuit current filament in MOSFET-Mode IGBTs," Proc. ISPSD 2016, pp. 319–322.
- [10] Sentaurus<sup>TM</sup> Device User Guide, Version Q-2019.12, Synopsys, Dec. 2019, pp.431–432.
- [11] Sentaurus<sup>TM</sup> Device User Guide, Version Q-2019.12, Synopsys, Dec. 2019, pp.1049–1324.
- [12] T. Ogura, H. Ninomiya, K. Sugiyama and T. Inoue, "Turn-Off Switching Analysis Considering Dynamic Avalanche Effect for Low Turn-Off Loss High-Voltage IGBTs," IEEE Transactions on Electron Devices, Vol. 51, No.4, April 2004, pp. 629–635.
- [13] M. Tsukuda, I. Omura, Y. Sakiyama, M. Yamaguchi, K. Matsushita and T. Ogura, "Critical IGBT Design Regarding EMI and Switching Losses," Proc. ISPSD 2008, pp. 185–188.